

**DRAFT**  
**Ion Figuring Thermal Considerations**

**Jerry Nelson**

**2010 March 28**

1	Introduction.....	2
2	Ion figuring Basics.....	2
3	Basic Properties of the Mirror Material.....	2
4	Elementary Model of a Glass Removal Algorithm.....	3
4.1	Gaussian Removal.....	3
4.2	Simple Removal Algorithm.....	8
4.2.1	Example: constant thickness removal.....	9
4.2.2	Non-uniform thickness removal.....	10
5	Time Averaged Thermal Expectations and Radiation.....	10
5.1	Small object radiating into a large cavity.....	10
5.2	Limiting size of object with maximum allowed temperature.....	11
5.3	Large object radiating inside a small cavity.....	11
5.4	Average temperature rise.....	11
5.5	Average front to back temperature difference.....	13
6	Time Dependent Heating.....	14
6.1	Local heating influence function.....	14
6.2	Local heating with no motion.....	15
6.3	Local heating when the beam is moving.....	17
6.4	Scan Pattern.....	20
7	Comparison with Finite Element Analysis.....	22
7.1	Heat dumped at the surface, Gaussian distribution.....	22
7.2	Power Deposited at Surface, Resulting Surface Heating.....	23
8	Summary.....	24

# 1 Introduction

TMT may ion figure the mirror segments after polishing in order to achieve the final desired optical surface. Here we carry out some thermal calculations to estimate the heating of the mirror that may occur from this ion figuring.

Ion figuring sends a high-energy beam of Argon atoms onto the mirror surface and atoms are ablated away by the particle collisions. The beam is closely Gaussian in shape and for a given desired removal map, the beam is raster scanned across the mirror surface with varying speeds used to control the amount of material removed. The power in the beam is not varied, only the translational speed.

The ion beam will add heat to the mirror, and the mirror will lose heat by radiation to the walls of the vacuum chamber that houses the mirror and ion gun. There will be both local heating as the ion beam scans over the mirror, and also average temperature changes as the mirror comes into a steady state balance between the power in and power out.

## 2 Ion figuring Basics

Assuming the following ion figuring system basic parameters: particleArgon ( $Z = 18$ ,  $A = 39.95$ )

mass of Argon atom	$6.63 \times 10^{-26}$ kg
kinetic energy per particle E	1400 eV
	$2.24 \times 10^{-16}$ J
atom velocity	$8.23 \times 10^4$ m/s
angle of incidence to surface	$90^\circ$
total beam power	126 W
beam intensity	$5.63 \times 10^{17}$ particles/second
Gaussian beam profile $\sigma$	0.025 m
effective area of Gaussian	$2\pi\sigma^2 = 3.93 \times 10^{-3}$ m <sup>2</sup>
central beam flux R	$3.21 \times 10^4$ W/m <sup>2</sup>
	$1.43 \times 10^{20}$ particles/m <sup>2</sup> /s
	1.43 particles/Å <sup>2</sup> /s
removal rate	$5.12 \times 10^{-12}$ m <sup>3</sup> /s (calibrated on Zerodur)
	(uncertain by a factor of 2)
maximum motion rate	0.25m/s

The ions are accelerated and after acceleration they are neutralized so the net beam is neutral and it is expected that individual atoms hitting the surface are also typically electrically neutral.

## 3 Properties of the Mirror Material

We expect to use a glass ceramic mirror material. Although several kinds are available, they have similar properties, and here we use the properties of Zerodur as being representative. Zerodur, is a carefully engineered mixture of compounds, and its low coefficient of thermal

expansion derives from it being about 70% crystalline and about 30% vitreous. Achieving this requires a carefully controlled thermal history, with much of the crystal growth occurring in the 700 °C region. The crystals ( $\beta$  quartz) have a negative coefficient of thermal expansion in the region of room temperature and the vitreous part has a positive coefficient of expansion (Duke and Chase, 1968). The crystals are typically about 50nm in size (Bennett et al, 1984), leading to a fairly transparent material. Zerodur is made of about 55% SiO<sub>2</sub>, 25% Al<sub>2</sub>O<sub>3</sub>, 8% P<sub>2</sub>O<sub>5</sub>, and miscellaneous other compounds. Its physical properties are:

density $\rho$	$2.53 \times 10^3 \text{ kg/m}^3$
elastic modulus E	$9.1 \times 10^{10} \text{ N/m}^2$
Poisson's ratio $\nu$	0.24
coefficient of thermal expansion $\alpha_\tau$	$< 1.0 \times 10^{-8} / ^\circ\text{C}$
thermal conductivity k	$1.64 \text{ W/m}^\circ\text{C}$
specific heat c	$821 \text{ J/kg}^\circ\text{C}$
thermal diffusivity $\alpha = k/c\rho$	$7.90 \times 10^{-7} \text{ m}^2/\text{s}$
transmission ( $\lambda > 5\mu\text{m}$ )	0, emissivity $\sim 1$
TMT segment diameter	1.44m
TMT segment thickness	0.045m

At this density, the typical distance between atoms in the glass is about 0.24nm. The average binding energy of the atoms in the glass is of order 1eV.

## 4 Elementary Model of a Glass Removal Algorithm

For the simplest removal algorithm we assume that the spatial frequencies in the error surface are only of very low spatial frequency. This means that the error surface has no errors that are of the same scale as the 25mm width of the ion beam removal profile. When only low spatial frequencies are involved, we can simplify the removal algorithm to one that says that the gun velocity is inversely proportional to the material to be removed. We further assume that the actual gun moves in a raster pattern over the mirror, so its motion is continuous in one direction (we call this direction X) and discrete in the other direction (we call this direction Y).

### 4.1 Gaussian Removal

It is useful to understand what spacing pattern in the raster scan is needed to make a smooth surface. Clearly if the rasters are too far apart one will get distinct grooves and not a smooth surface. Hence we review the pattern implications for the simplest removal pattern, a uniform reduction of thickness.

Assume that the raster pattern spacing is  $u$ . Given the width of the Gaussian removal profile we want to understand the amplitude of the residual scalloping that the raster makes as a function of  $u$ . We define a Gaussian as

$$h(x) = \frac{1}{\sqrt{2\pi}\sigma} e^{-\frac{(x-x_0)^2}{2\sigma^2}} \text{ for a one dimensional Gaussian} \quad (1)$$

$$h(x,y) = \frac{1}{2\pi\sigma^2} e^{-\frac{(x-x_0)^2}{2\sigma^2}} e^{-\frac{(y-y_0)^2}{2\sigma^2}} \text{ for two dimensions}$$

These are normalized so their integral over the variables is 1.

Figure 1 shows a set of one dimensional Gaussians separated by  $1.5\sigma$ .

**7 individual Gaussians separated by the raster spacing of 1.5 sigma**

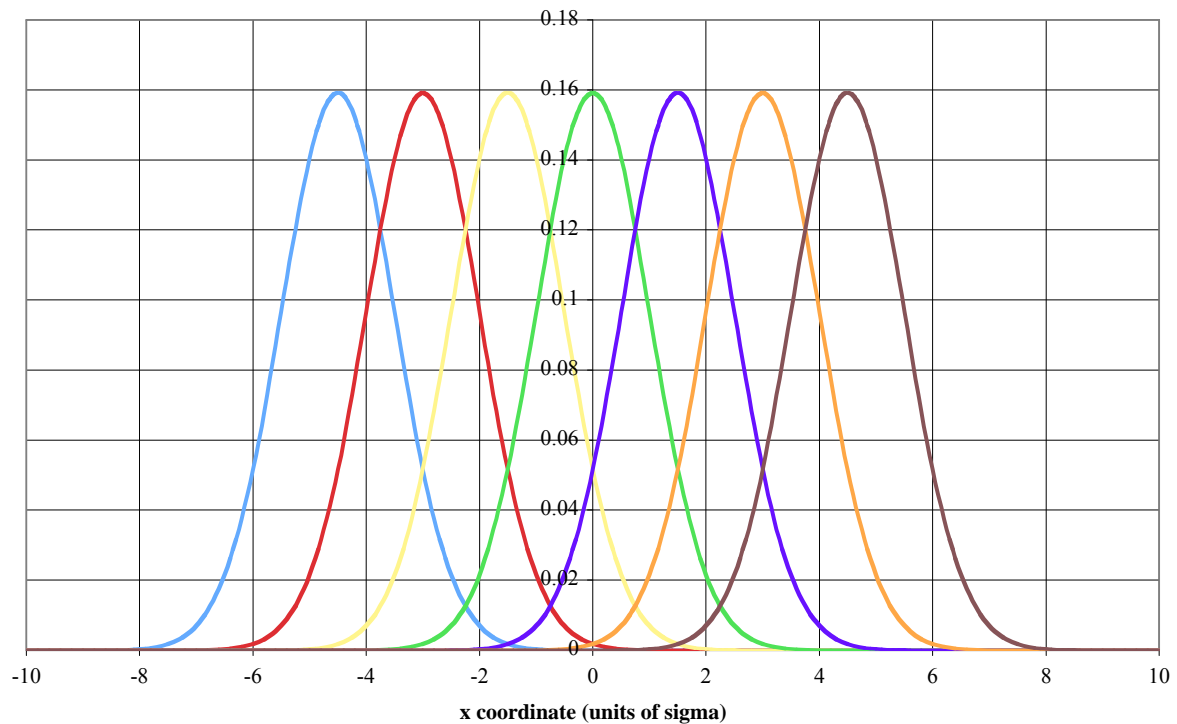


**Figure 1:** 7 Gaussian beams separated by  $1.5\sigma$

Using units of  $\sigma$ , we can ask what such a sum of Gaussians is, as a function of  $u$  (in units of  $\sigma$ ). We give an example in Figure 2 with scans starting at  $x=0$  and stepping in units of  $2.5\sigma$ .

### Net Removal ( $u=2.5\sigma$ )

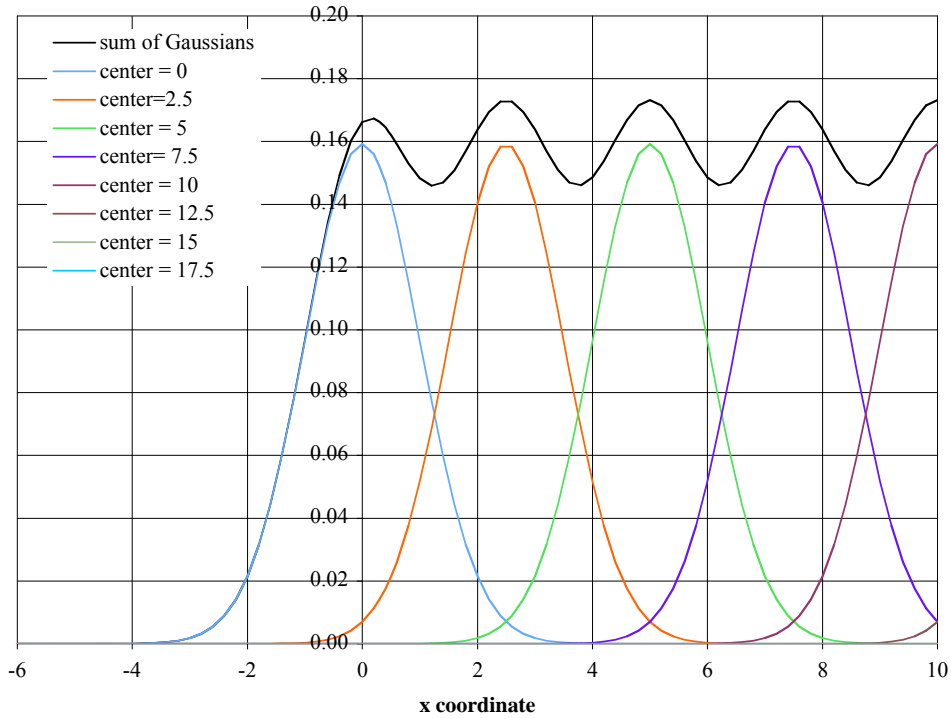


**Figure 2:** the sum of Gaussians starting at  $x=0$  and going in steps of  $2.5\sigma$ . Note that the fluctuations in the sum are relatively small.

As the raster interval  $u$  becomes smaller, the sum of the Gaussians becomes smoother very rapidly. In Figure 3 we show the ripple size as a function of spacing where we are plotting  $(\text{peak-valley})/\text{peak}$ .

Note also that the leading edge is essentially defined by the first raster.

### Ripple for summing Gaussians

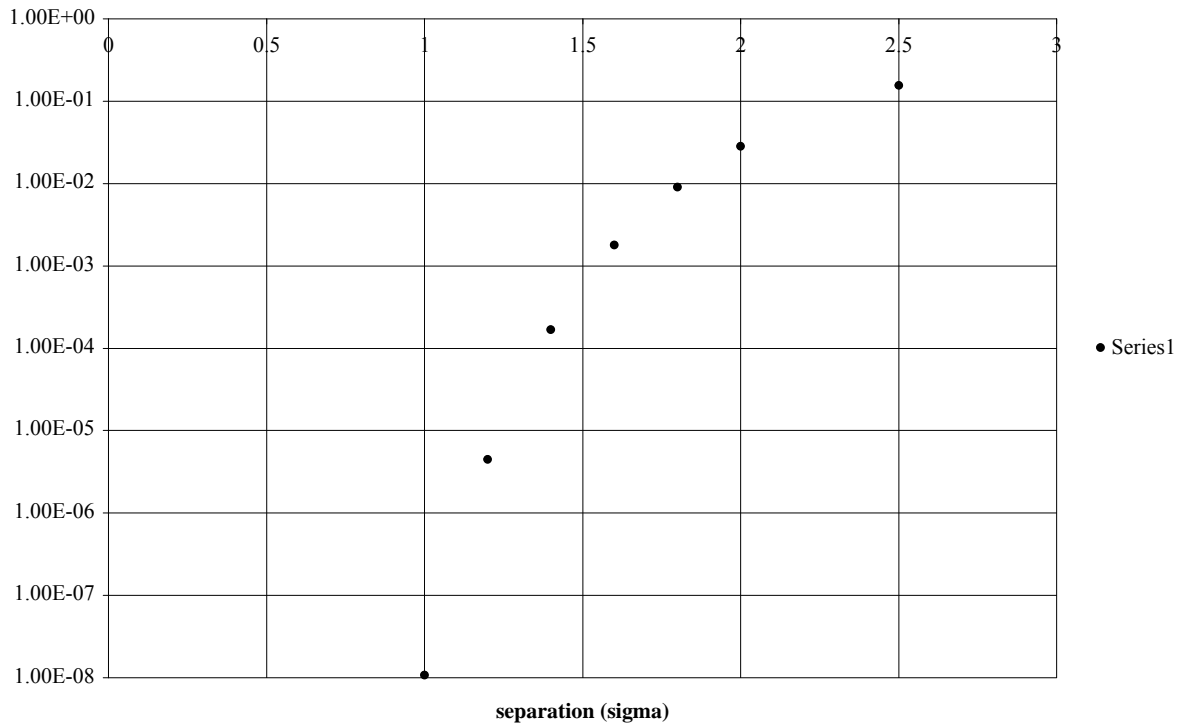


**Figure 3:** The size of the ripple in the sum of Gaussians. Plotted is (peak-valley)/peak. Note that the vertical scale is logarithmic. The fractional size of the ripple becomes negligible very rapidly as the Gaussian peaks become closer together.

One can see from this figure that for all practical purposes, raster separations of  $1.5\sigma$  are sufficiently fine, with fractional ripple smaller than 0.001. Figure 4 shows the ripple for this spacing.

### Net Removal ( $u=1.5\sigma$ )

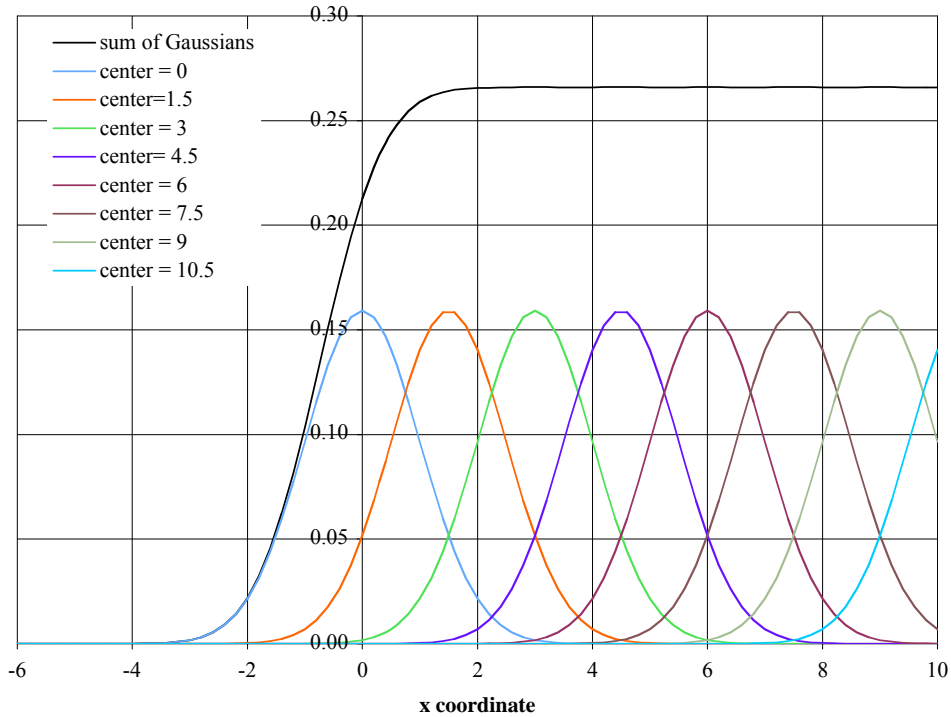


**Figure 4:** the Gaussians and the sum for spacing of  $u=1.5\sigma$  starting at 0.

From this analysis one can see that there is no theoretical advantage in making the raster interval any smaller than  $1.5\sigma$ . Denser scans are not harmful of course, but the ion head must travel faster for a given desired net removal.

To bolster our intuition, we consider an example showing how the net removal is achieved for each of the scans that contribute to the net removal. The net removal at  $x=3$  in Figure 4 consists of removals from each raster:

**Raster peak removal at  $x=3$**

0	0.0018
1.5	0.0517
3.0	0.1592
4.5	0.0517
6.0	0.0018
7.5	6.4e-6

As expected, only a few Gaussian rasters actually contribute in any significant way to the net removal. Only 3 rasters are above 1% of the net removal. As the rasters get closer together, more rasters will contribute to the net removal at a given point. The maximum fraction of the

total removal that a single scan contributes we call  $\beta$ . This gets smaller as the scans become closer. For scans  $1\sigma$  apart  $\beta=0.4$ .

This can be seen systematically as a function of the scan interval in Figure 5, which shows the depth of the Gaussian for a single scan/the net removal from all of the nearby scans.

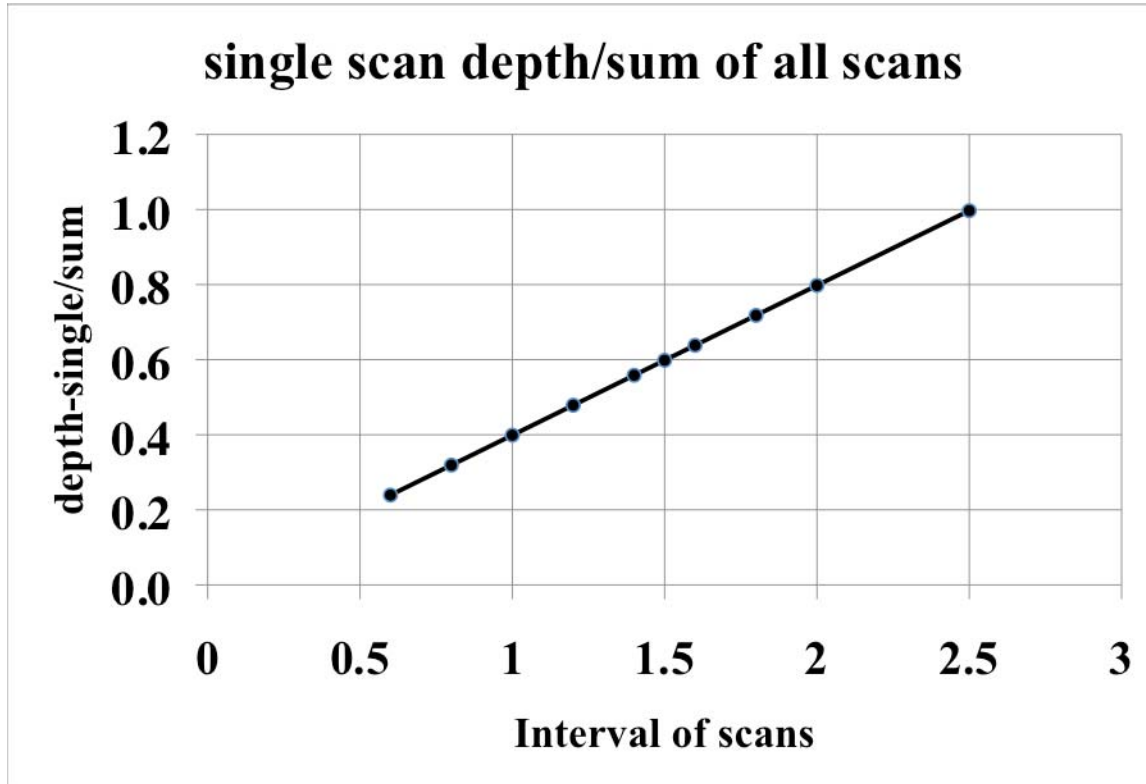


**Figure 5:** depth of a single scan in its center divided by the sum of removal at that point from all nearby scans. As scans get closer together, each scan removes a smaller fraction of the total removed material. Scan interval is in units of  $\sigma$ .

Note that the relationship shown in Figure 5 appears linear. It can be shown that in the limit of small scan interval (interval  $< \sim 2\sigma$ ) the sum of all scans  $S$  satisfies  $\beta = \frac{1}{S} = u/\sigma\sqrt{2\pi}$ . This is within 2% for  $u/\sigma = 2$ , and within 0.1% for  $u/\sigma = 1.5$ , and essentially perfect for smaller values of  $u/\sigma$ .

Another point to note is that the 2-dimensional Gaussian is a separable function, that is, it can be written as a product of a function in  $x$  and a function in  $y$ . This is not generally true for 2-dimensional axisymmetric functions. When it is true, the removal profiles become the one-dimensional profiles, and net removal over two dimensions is much simpler to calculate.

## 4.2 Simple Removal Algorithm

The removal rate for a stationary beam centered at the origin is given by

$$\frac{dz(x,y)}{dt} = \frac{\dot{V}}{2\pi\sigma^2} e^{-\frac{r^2}{2\sigma^2}} = \dot{V} \frac{e^{-\frac{x^2}{2\sigma^2}}}{\sqrt{2\pi}\sigma} \frac{e^{-\frac{y^2}{2\sigma^2}}}{\sqrt{2\pi}\sigma} \quad (2)$$

Where  $dz/dt$  is the removal rate at the point  $x,y$

$\dot{V} = dV/dt$  is the bulk removal rate of the ion beam =  $5.12e-12m^3/s$

$\sigma$  is the Gaussian width of the beam removal pattern

We assume that the ion gun is moving in a boustrophedonic pattern, so the beam moves continuously along  $x$  and step wise along  $y$ . Since the removal shape is closely Gaussian, we can use the above Gaussian analysis. For surface removal shapes that vary slowly in  $x$  and  $y$  compared to  $\sigma$ , we can determine the desired velocity of ion gun along  $x$ . We assume that the power in the gun is unchanged, and that only speed changes are used to modify the removal of material. Assume we want to remove a height  $z(x,y)$ . As the beam moves past a given point, we should integrate the Gaussian profile in the  $x$  direction to get the net removal. Thus we integrate over  $x=vt$ , and integrate over all  $t$  to obtain (using the normalization of a Gaussian)

$$h = \frac{\dot{V}}{v\sqrt{2\pi}\sigma} e^{-\frac{y^2}{2\sigma^2}} \quad (3)$$

and since the desired  $h$  is

$$\beta z(x,y) = h \quad (4)$$

we obtain (using the formula for  $\beta$  from the previous section)

$$v(x,y) = \frac{\dot{V}}{uz(x,y)} \quad (5)$$

and  $z(x,y)$  is the desired removal shape.

Note that (5) does not contain  $\sigma$ . A wider beam profile implies material is removed over a wider footprint, with less removed at a given point. On the other hand more scans contribute to removal at a given point. As a result, the two effects cancel and  $\sigma$  does not enter into the velocity calculation.

#### 4.2.1 Example: constant thickness removal

Assume we want to remove a uniform thickness  $z(x,y)=0.5\mu m$ . Assume that the scan lines are separated by a width  $u=\sigma$ . We determine the gun speed in two different ways.

Method 1: Using (5) we calculate  $v(x,y)=4.10e-4$  m/s

Method 2: Note that the bulk removal is  $Area \cdot z$ . The time needed to removal this material is thus  $t = \frac{Az}{\dot{V}} = 9.77e4$  s/m<sup>2</sup>. For a TMT segment with  $Area=1.35m^2$  the needed scan time is 36.6

hours. For a scan with  $u=0.025m$ , the total scan length will be  $Area/u = 40m/m^2$ , and a resulting speed  $v(x,y)=4.09e-4$  m/s.

Thus two different methods give the same result.

We note that the minimum velocities are small, 0.4mm/sec. As we will see, this may cause unacceptable heating of the glass. One can achieve the same removal by moving the gun faster and making many passes over the glass. This does not reduce the heat load, but it allows it to be distributed more uniformly. We will explore this in more detail in later sections.

## 4.2.2 Non-uniform thickness removal

When the material to be removed is non-uniform in thickness, there will be variable speeds, according to (5). For slowly varying heights, (5) is an adequate basis for the gun speed. As the shape variations become spatially more variable, and adjacent scans will be at slightly different speeds, thus influencing the actual removal at a given spot. Such errors can be corrected by using deconvolution to determine the optimal speed at any point, thus including the desired global removal pattern in the calculation of the speed at any point. For removal variations that can be approximated by a linear variation over the non-zero part of the beam removal pattern ( $\sim 2\sigma$  in size) no corrections are needed. Only significant local curvature will impact the removal algorithm. A more detailed discussion of optimized removal algorithms will be discussed in a separate document.

As noted in 4.2.1 one might use multiple passes and move the gun at higher speeds. Given a maximum speed limit of 0.25m/s, such a strategy will reduce the dynamic range of removal. This dynamic range is the ratio of the maximum gun speed to the minimum gun speed used.

## 5 Time Averaged Thermal Expectations and Radiation

We expect that the typical segment will have  $1\mu\text{m}$  peak to valley errors upon entering ion figuring. This means that on average  $0.5\mu\text{m}$  of material will be removed. With a mirror area of  $1.35\text{ m}^2$  we expect the average removal volume will be  $6.73 \times 10^{-7}\text{ m}^3$ . Thus an average segment will require  $1.32 \times 10^5\text{ s}$  or 36.5 hours of ion figuring time, ignoring ion polishing iterations and excess removal due to beam runs carried out at higher than minimum gun speed.

With power coming into the mirror at 126W, over time the mirror will heat up and continue to do so until its net radiated power is 126W. Since the ion figuring is carried out in a vacuum chamber, there is no convective cooling. Given the mirror is supported only minimally, conductive cooling will also be negligible.

We now calculate the radiative losses for some simple cases.

### 5.1 Small object radiating into a large cavity

When the mirror is small compared to the vacuum chamber, the net radiated power is given by

$$P = A\varepsilon\sigma(T_{\text{mirror}}^4 - T_{\text{wall}}^4) \quad (6)$$

where  $A$  is the area of the mirror

$\varepsilon$  is the emissivity of the mirror ( $\sim 1$  for Zerodur at  $\lambda > 5\mu\text{m}$ )

$\sigma$  is the Stefan-Boltzman constant  $5.67 \times 10^{-8}\text{ W/m}^2/\text{K}^4$

$T_{\text{mirror}}$  is the steady state temperature of the mirror

$T_{\text{wall}}$  is the temperature of the walls of the large vacuum chamber

This formula is valid when the re-radiation or scattering from the walls only rarely hits the mirror. In this limit the emissivity of the container walls is unimportant.

For the average beam power of 126W, a surface area of  $2.89\text{m}^2$ , and an assumed wall temperature of  $293\text{K}$ ; the steady state mirror temperature will be  $T_{\text{mirror}} = 300.4\text{K}$  or about

7.4°C warmer than the wall temperature. This temperature increase is quite modest, and not a problem for the glass properties or for any adhesives on the back of the mirror.

## 5.2 Limiting size of object with maximum allowed temperature

We can solve a closely related problem, where the allowed temperature rise is given and we calculate the size of the radiating object. The adhesive we plan to use for attaching the SSA to the mirror segment is Scotch-Weld Epoxy 2216. We want to limit its temperature to below 70°C or 343°K.

For  $T_{\text{mirror}} = 70^\circ\text{C}$ ,  $A=0.343\text{m}^2$  or since both sides radiate, a square 0.42m on a side. Thus if we want to limit the temperature rise to 70°, we need to find a way to distribute the heat load uniformly over a region at least as large as 0.42m on a side, in order for radiative coupling to the walls of the ion chamber to limit the temperature rise to the allowed level. Put another way, if an object 0.42m on a side had an infinite internal thermal conductivity, then the IBF heat load would not heat it up beyond our 70° limit. An object with finite conductivity that meets our max temperature will need to be larger than this.

## 5.3 Large object radiating inside a small cavity

In this example the object size is not negligible compared to the chamber. In this case the emissivity of the walls of the chamber become important. The results depend on the geometry since the fraction of the wall radiation/scattering hitting the object becomes important. One can write an approximate solution as

$$P = \frac{\sigma A_1 (T_{\text{mirror}}^4 - T_{\text{wall}}^4)}{1/\varepsilon_{\text{mirror}} + (1/\varepsilon_{\text{wall}} - 1)(A_{\text{mirror}}/A_{\text{wall}})} \quad (7)$$

This reduces to (6) when  $A_{\text{mirror}}/A_{\text{wall}}$  goes to zero.

As an example, assume the ion figuring chamber is 2mx2mx2m. Thus the wall area is  $A_{\text{wall}} = 24\text{m}^2$ . If the emissivity of the wall is low, such as would occur with aluminum foil covering the walls ( $\varepsilon_{\text{foil}} = 0.03$ ), the denominator is  $\sim 4.9$  so the radiant efficiency is reduced by a factor of 5! In this case the steady state temperature of the mirror is 325°K, or 32°C warmer than the walls.

Clearly low emissivity walls are a poor choice when effective radiative transfer is desired.

Stainless steel, unless it has been polished, has  $\varepsilon=0.5$  and in equation (7) one sees that the finite size of the chamber is unimportant ( $T_{\text{mirror}} = 301.2^\circ\text{K}$ ), and equation (6) can be used.

Assuming a TMT chamber of 10'x10'x7', a surface area of 44.6m<sup>2</sup>, and an emissivity of 0.7, the denominator is 1.03 using (7). Therefore, this chamber is almost radiatively coupled to the segment perfectly.

## 5.4 Average temperature rise

If we apply power to the front surface of a mirror, the mirror surface will heat up and this heat will diffuse through to the back of the mirror. If the thermal conductivity is large enough, the mirror will heat up uniformly. In this case

$$\frac{dT}{dt} = \frac{P}{cM} \quad (8)$$

where  $P=126\text{W}$

$$c=821 \text{ J/kg}^\circ\text{C}$$

$$M=153\text{kg}$$

$$\text{Or } \frac{dT}{dt} = 1.00\text{e} - 3^\circ/\text{s}$$

This it would take  $\sim 7400\text{s}$  to heat the mirror up the  $7.4^\circ$  that represents the radiative balance we saw with equation (6). This time (2.0 hrs) is small compared to the estimated 36 hours of ion figuring time for our estimated typical segment. Thus we expect to reach the radiative steady state if we can distribute the heat input uniformly enough.

If we explicitly include the radiative cooling in the equation, we get

$$\frac{dT}{dt} = \frac{(P_{IBF} - P_{rad})}{cM} = \frac{(P_{IBF} - A\varepsilon\sigma(T^4 - T_{wall}^4))}{cM} \quad (9)$$

This can be solved for small temperature differences to get the response vs time. This can be written as

$$T(t) = T_w + \frac{P}{4A\varepsilon\sigma T_w^3} (1 - \exp(-\frac{4A\varepsilon\sigma T_w^3}{cM} t)) = 293 + 7.64(1 - \exp(-t/7620)) \quad (10)$$

This temperature growth to equilibrium is shown in Figure 6.

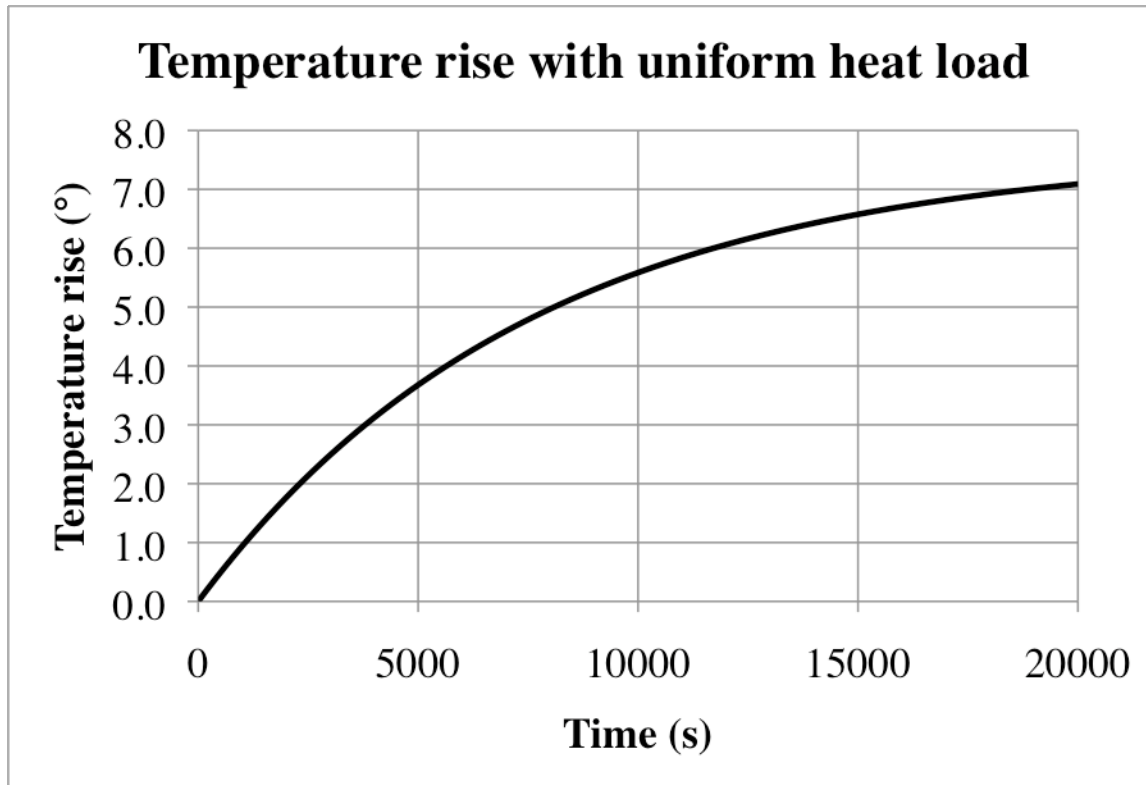


**Figure 6** The temperature rise of a TMT segment uniformly heated and subject to radiative cooling to the wall of the IBF chamber.

### 5.5 Average front to back temperature difference

The heat is deposited onto the front surface. How long does it take for the heat to get to the back surface and what is the front to back temperature difference? Again, assume we are applying the heat evenly over the front surface. The incident power will both radiate and conduct through to the mirror back, and the back will radiate. Thus the front and back temperatures will be different

$$\begin{aligned}
 P &= A\sigma(T_1^4 - T_{\text{wall}}^4) + A\sigma(T_2^4 - T_{\text{wall}}^4) \\
 P &= A\sigma(T_1^4 - T_{\text{wall}}^4) + \frac{Ak}{h}(T_1 - T_2)
 \end{aligned}
 \tag{11}$$

we want to solve these two equations for  $T_1$  and  $T_2$ . We solve these numerically to obtain

$$T_1 = 301.5 \text{ (8.5° above } T_{\text{wall}})$$

$$T_2 = 300.22 \text{ (1.28° cooler than the front surface)}$$

$$P_{\text{conduction}} = 58 \text{ W} = P_{\text{rad from back surface}} \text{ (} P_{\text{rad from front surface}} = 68 \text{ W)}$$

We conclude that when the heat load is uniform the temperature difference front-back is small, and both sides radiate similar amounts.

Unfortunately, these average values may not represent the dynamic heating from a localized ion beam that is moving along the front surface.

## 6 Time Dependent Heating

We now turn to details of the heating of glass due to the local deposition of energy from the ion beam. We will be solving the heat equation. Since this is a linear equation, any solutions we find can be added and the sum will be a solution of the problem. Thus, with suitable care to details, we can find solutions and then integrate them over time to find additional solutions.

Since the ion beam is moving across the mirror, the heating effects are locally time dependent. Where the beam is at a given instant will be subject to the greatest heating, but the heat diffuses through the mirror, so on some time scales and distances the local temperature will depend on the temporal and spatial distribution of the heat source. This is a complex problem, and we will generate a few simple cases that are analytically accessible to get a feeling for the magnitude of the effects.

There are three issues associated with local heating:

If the material heats up too much, the low thermal expansion properties of the Zerodur may be permanently altered and this may change the shape of the mirror. Generally temperatures above 100°C are at risk of changing the material properties.

If the local heating exceeds about 70°C where epoxy joints are located, the epoxy will temporarily weaken and if the joints are loaded, they may break.

If the local heating exceeds about 100°C where epoxy joints are located, the epoxy may be permanently weakened.

As a result of these concerns, we will set an upper temperature limit of 70°C in developing a suitable plan for IBF.

### 6.1 Local heating influence function

A point source of thermal energy deposited at the surface of a plane at  $t=0$  will heat the half space according to (see Landau and Lifshitz, **Fluid Mechanics**, Vol 6, p200)

$$T(r,t) = \frac{2Q_0}{8\pi^{3/2}c\rho\alpha^{3/2}t^{3/2}} \exp\left[-\frac{r^2}{4\alpha t}\right] \quad (12)$$

Where  $Q_0$  is the deposited energy at the origin

$c$  is the specific heat

$\rho$  is the density

$\alpha$  is the material diffusivity

$r$  is the distance from the origin

In this model the temperature near the origin is arbitrarily large. However, this is essentially the point source sensitivity and we will develop upon this. It is easy to show by integration that (12) satisfies conservation of energy over all time.

Our actual heating function is a Gaussian in  $x,y$ , not a single point. Thus we must convolve (12) with the beam Gaussian. Noting that convolving two Gaussians produces a Gaussian with a variance equal to the sum of the initial variances, we can rewrite (12) as

$$T(r,t) = \frac{2Q}{8\pi^{3/2}c\rho\alpha^{3/2}t^{3/2}} \exp\left[-\frac{r^2}{4\alpha t}\right] = \frac{2Q}{c\rho} \frac{1}{(2\pi\sigma_i^2)^{3/2}} \exp\left[-\frac{x^2 + y^2 + z^2}{2\sigma_i^2}\right] \quad (13)$$

where  $\sigma_i^2 = 2\alpha t$

The convolution with the ion beam shape (Gaussian in x and y) thus yields

$$T(r,t) = \frac{2Q}{c\rho} \frac{1}{(2\pi(\sigma_i^2 + \sigma^2))\sqrt{2\pi}\sigma_i} \exp\left[-\frac{x^2 + y^2}{2(\sigma_i^2 + \sigma^2)}\right] \exp\left[-\frac{z^2}{2\sigma_i^2}\right] \quad (14)$$

The lateral characteristic size is  $\sim \sigma$  when t is small, and  $\sim \sqrt{2\alpha t}$  when time is large. When  $\sigma^2 = 2\alpha t$  we see there is a characteristic lateral diffusion time constant

$$t_c = \frac{\sigma^2}{2\alpha} = 396 \text{ sec} \quad (15)$$

This is the characteristic time the lateral diffusion of heat occurs over the same size as the beam Gaussian size, given our Gaussian beam profile.

Another time constant, the time it takes for the front heat load to heat the back surface of a plate of thickness h is given by

$$t_h = \frac{4h^2}{\pi^2\alpha} = 1039 \text{ s}$$

## 6.2 Local heating with no motion

Consider a simple limiting case where the ion beam is stationary in one place. It will gradually add energy to the glass and the glass will heat up. However, the heat will diffuse as well, driven by the temperature gradients. Thus we expect that there will be a limiting temperature rise. We assume a half space of glass, so this is not necessarily a realistic problem for our mirror segments.

We want the temperature at the center of the beam at the surface of the glass (0,0,0). Note that  $dQ/dt=P$ , and integrate (14)

$$T(0,t) = \frac{2P}{c\rho(2\pi)^{3/2}} \int_0^t dt \frac{1}{(\sigma_i^2 + \sigma^2)\sigma_i} = \frac{2P}{c\rho(2\pi)^{3/2}} \int_0^t dt \frac{1}{(2\alpha t + \sigma^2)\sqrt{2\alpha t}} = \frac{2P \tan^{-1}(\sqrt{2\alpha t}/\sigma)}{c\rho(2\pi)^{3/2}\alpha\sigma} \quad (16)$$

This is plotted in Figure 7.

For small times this simplifies to

$$T(0,t) = \frac{Pt^{1/2}}{\pi^{3/2}c\rho\alpha^{1/2}\sigma^2} \quad (17)$$

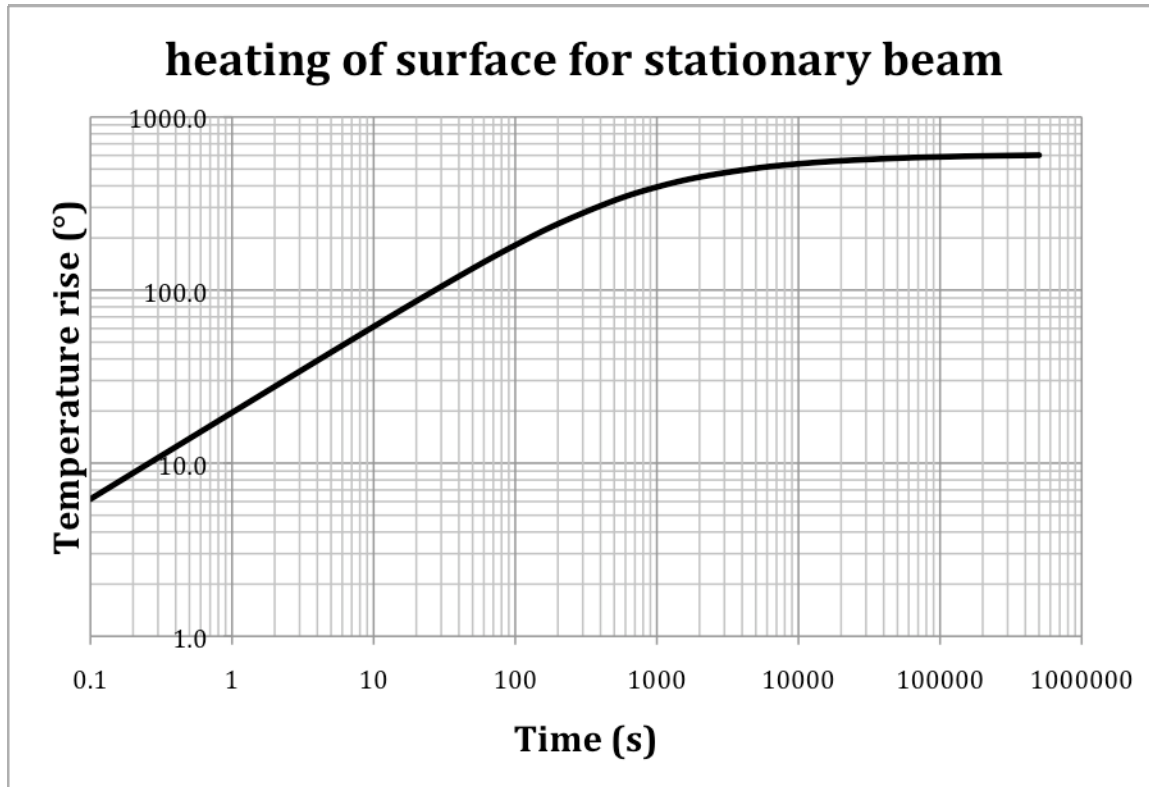


**Figure 7** The temperature rise at the center of the ion beam impinging on a half space of glass. Note the characteristic time matches (15). For our constraints, we can tolerate a rise of 50°C which is reached in about 7 seconds.

We see that as expected the temperature rises as  $t^{1/2}$ , then levels off. The time constant is set by (15). For our allowed temperature rise from 20°C to 70°C the beam can only be on for about 7 sec. For a moving beam, the above result is approximately correct when the beam has moved  $< 1\sigma$ . Thus we see that the minimum beam speed we can tolerate without overheating the glass is about 3.6e-3m/s. This is about 10x the rate we found in 4.2.1 for our example removal of 0.5µm.

For short times we can also determine the temperature rise in the vicinity of the beam. Going back to (14) we assume short times ( $\sigma_t^2 \ll \sigma^2$ ) to get

$$T(r,t) = \frac{2Q}{c\rho} \frac{1}{(2\pi\sigma^2)\sqrt{2\pi}(\sigma_t)} \exp\left[-\frac{x^2+y^2}{2\sigma^2}\right] \exp\left[-\frac{z^2}{2\sigma_t^2}\right] \quad (18)$$

and then integrate over time to get (for small times)

$$\begin{aligned} T(r,t) &= \frac{2P}{c\rho(2\pi)^{3/2}\sigma^2} \exp\left[-\frac{x^2+y^2}{2\sigma^2}\right] \int_0^t dt \frac{1}{\sqrt{2\alpha t}} \exp\left[-\frac{z^2}{4\alpha t}\right] \\ &= \frac{2P}{c\rho(2\pi)^{3/2}\sigma^2} \exp\left[-\frac{x^2+y^2}{2\sigma^2}\right] \left[ \sqrt{\frac{2t}{\alpha}} \exp\left[-\frac{z^2}{4\alpha t}\right] - \sqrt{\frac{\pi}{2\alpha^2}} z \left(1 - \operatorname{erf}\left(\frac{z}{\sqrt{4\alpha t}}\right)\right) \right] \end{aligned} \quad (19)$$

For times  $< 100$ s this is an excellent approximation. We show this temperature rise for a set of  $z$  values in Figure 8.

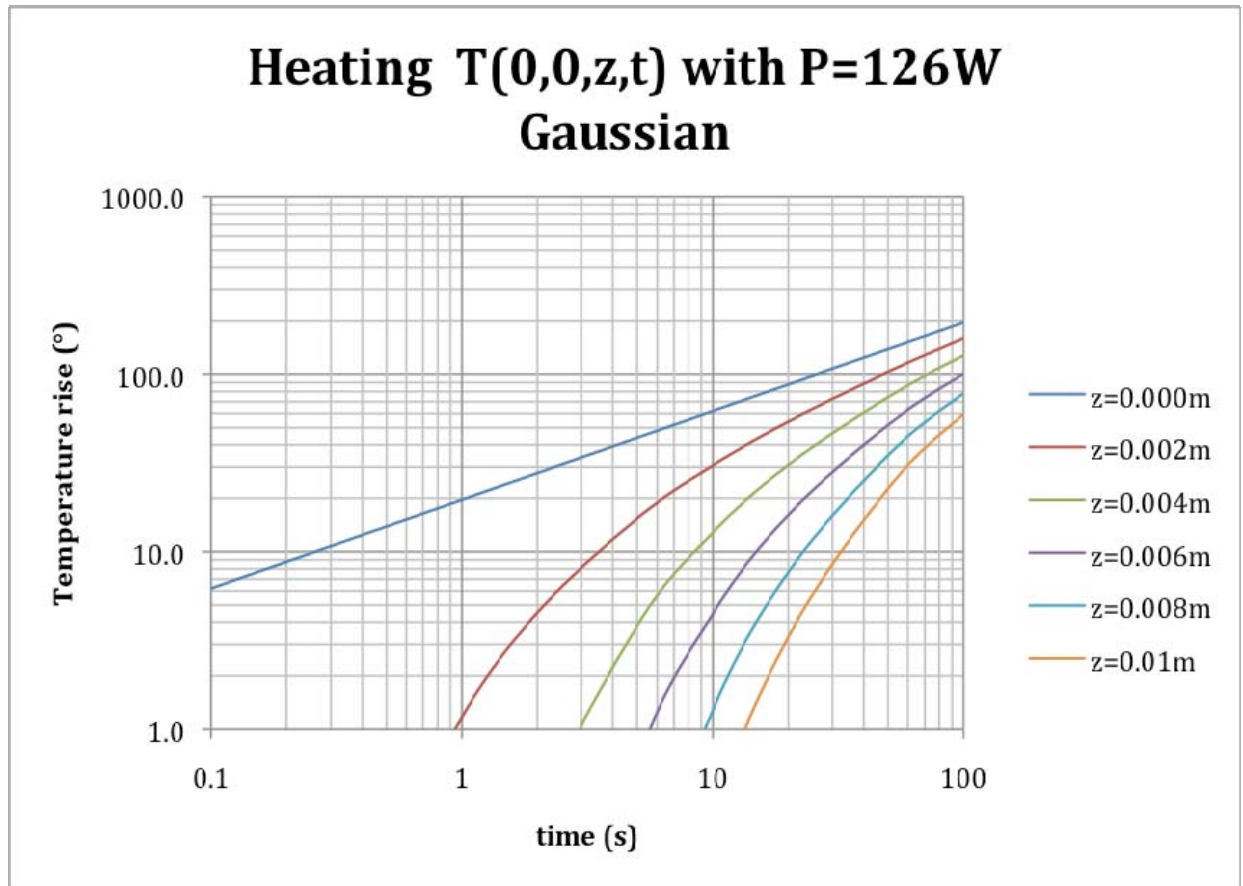


**Figure 8** The temperature rise vs time and  $z$  depth is shown for a stationary Gaussian power input at the top surface of  $P=126W$ . The curve at  $z=0$  is the same as the curve in Figure 7. Note the temperature rise vs  $z$  is quite modest for times  $<100s$ . For example, 10mm into the glass, the temperature rise after 100s is only  $60^\circ$  while the surface has risen  $200^\circ$ .

We see from this equation and the figures that for short times ( $t < 100s$ ) that the surface temperature rises with the same shape as the Gaussian heating function, and that it drops off rapidly with the depth. One consequence of this is that the actual thickness of the mirror is unimportant for our problems. Characteristic thicknesses for our problem are 20mm in the segment center, and 45mm for the rest of the mirror.

### 6.3 Local heating when the beam is moving

If the ion beam is moving along the surface as some speed  $v$ , then when  $vt_c = \sigma$  the beam motion will be moving as the same speed as the diffusion. This gives a speed below which we can assume the beam is stationary, for purposes of calculating the temperature. This is  $3.16e-5m/s$ . For our removal example of  $0.5\mu m$  we needed a speed of at least  $4.09e-4m/s$  (see 4.2.1). So our beam is moving rapidly compared to diffusion.

We saw in 6.2 that to avoid local overheating we needed to limit the beam duration to about 7sec. If the beam is moving, we expect that only if it moves a distance  $\sim \sigma$  in this time will local heating be acceptable, or  $v > 3.6e-3m/s$ , again much greater than diffusion.

Formally, we can calculate the temperature along the scan line by integrating (14), and noting that at a given instant the beam is centered at  $x=x_0+vt$ , and  $\sigma_t^2 = 2\alpha(t_0 - t)$ .

$$\begin{aligned}
T(r,t) &= \frac{2P}{c\rho} \frac{1}{(2\pi)^{3/2}} \int_0^{t_0} dt \frac{1}{(\sigma_t^2 + \sigma^2)(\sigma_t)} \exp\left[-\frac{x^2}{2(\sigma_t^2 + \sigma^2)}\right] \\
&= \frac{P}{(2\pi)^{3/2} c\rho\alpha\sigma} \int_0^{t_0/\mu_0} dw \frac{1}{(1+w)(\sqrt{w})} \exp\left[-\frac{(x - vt_0 + v\mu_0 w)^2}{2\sigma^2(1+w)}\right]
\end{aligned} \tag{20}$$

where we have set  $y=z=0$ , and the result is the temperature at  $x$  for a final time  $t_0$ . We assume the beam is turned on at  $t=0$ , and the initial position is  $x_0=0$ . We integrate (20) numerically to obtain our results. Numerical integration must be done carefully since the integrand becomes infinite at  $w=0$ . Noting that the exponential is bounded and slowly varying, we can analytically integrate the first term in the integrand and use that as we numerically carry out the integration. Note that

$$\int \frac{dw}{(1+w)(\sqrt{w})} = 2 \tan^{-1} \sqrt{w} \tag{21}$$

Figure 9 shows the temperature along the scan line after 40s of heating with the beam moving at  $v=0.005\text{m/s}$ . Since at any instant the beam is basically depositing a Gaussian heat pattern, it is interesting to see what the pattern of deposit is from any time interval. The figure also shows the temperature rise from the last second. This shows that the net temperature at a given position is due to the accumulated power from many positions as the beam moves along the  $x$  axis.

Note that there is an initial rise in temperature due to the fact that we turned on the beam at  $t=0$ ,  $x=0$ , so there is no heat from negative times. After about 0.05m the initial conditions are “lost” and the curve shows the attenuation due to thermal diffusion of the past energy deposited. As we approach the “present time” the temperature peaks, as diffusion is minimum, then the temperature rise decreases as we are simply seeing the impact of the Gaussian ion beam, but the center of the beam has not yet reached that location.

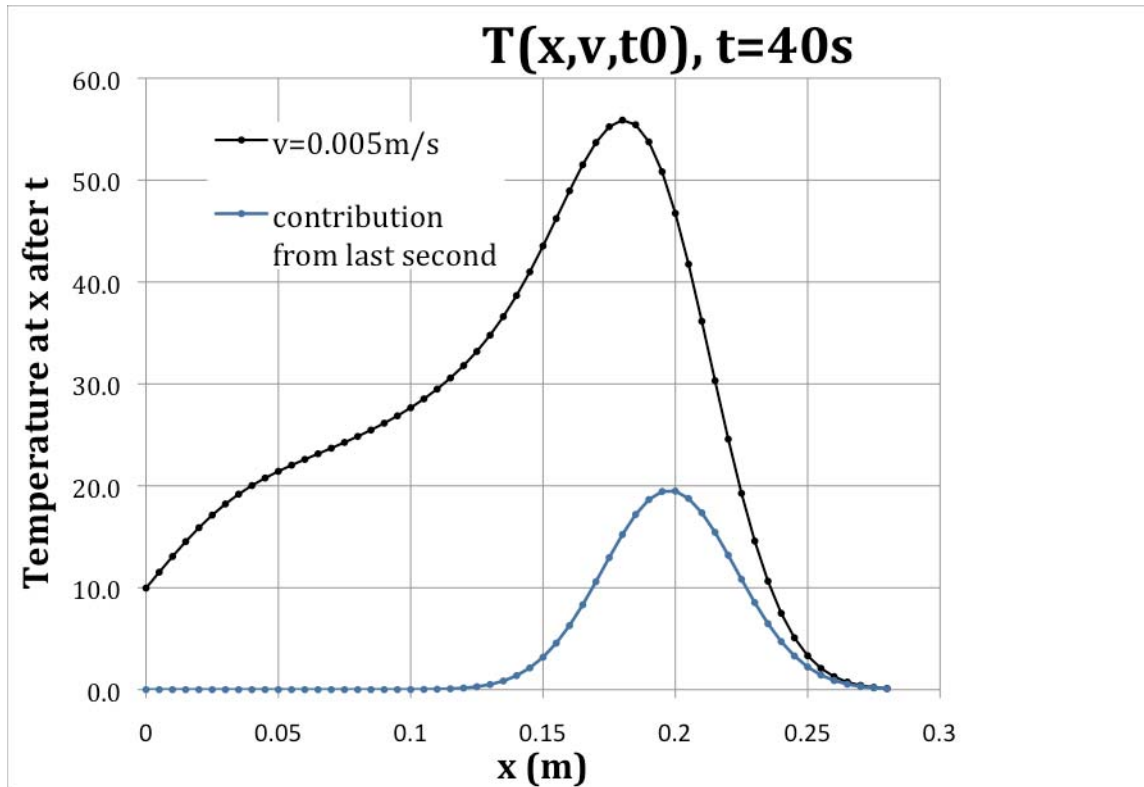


**Figure 9** The temperature rise along the beam scan line (along x). The beam is moving at  $v=0.005\text{m/s}$  and the temperature is given at the surface,  $y=z=0$ . The blue curve shows the temperature rise from the last second.

Our goal is to find the beam speed that limits the temperature rise to no more than  $50^\circ$ . Using (20) we can compute the maximum temperature for various scan speeds and we show this for several speeds in Figure 10. The maximum temperature varies as  $v^{-1/2}$ .

For our example of removing  $0.5\mu\text{m}$  of glass the required speed for removal all the material in a single scan pattern was  $4.1\text{e-}4\text{m/s}$  (section 4.2.1). Thus it is evident that we must carry out multiple scans to achieve this removal. For a lower limit scan speed of  $5\text{e-}3\text{m/s}$  achieving the desired removal will require 12 complete scans, assuming the individual scan lines are  $0.025\text{m}$  apart.

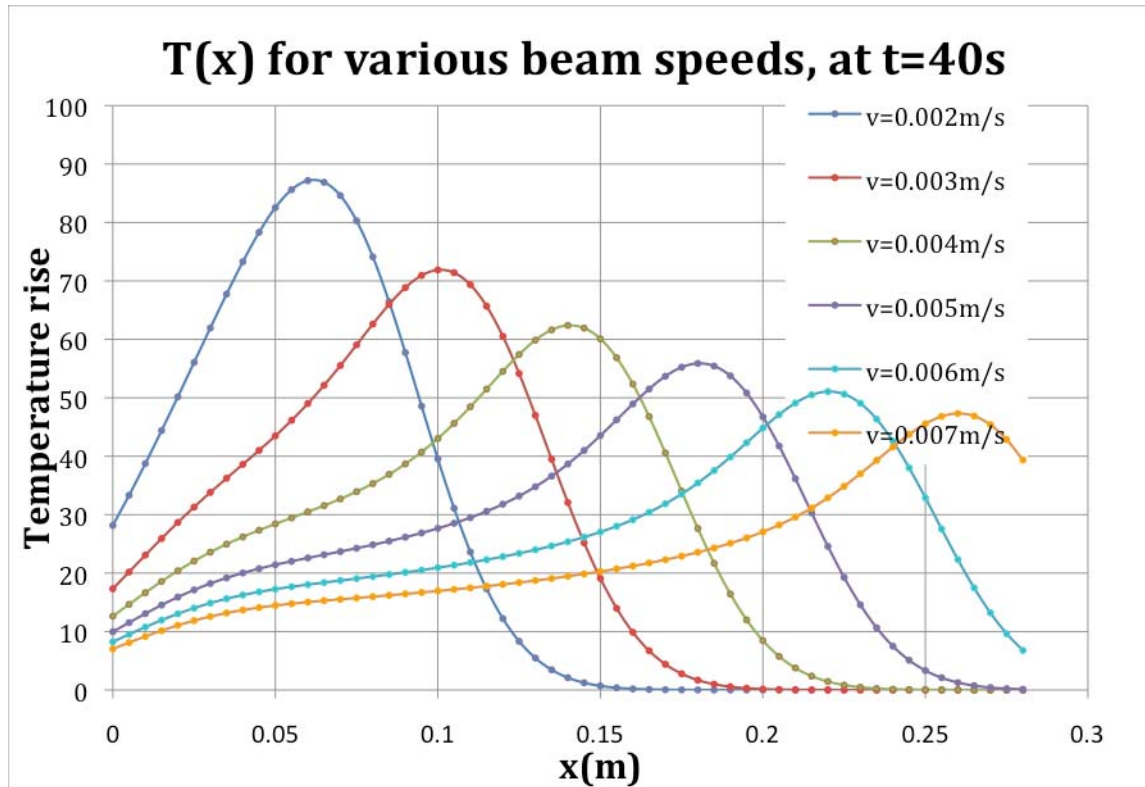


**Figure 10** The heating of the surface from scans at different speeds is shown. If we wish to keep the surface temperature rise below  $50^\circ$ , we must keep the scan speed above  $0.005\text{m/s}$ .

## 6.4 Scan Pattern

Since we want to minimize the heating of the glass we need to consider the impact of repeated scans, in particular consecutive scans. The segment is hexagonal, but for simplicity we will discuss a square segment with the same area of  $1.35\text{m}^2$ , or  $1.16\text{m}$  on a side.

At the rate of  $0.005\text{m/s}$  the beam will traverse the width of the segment in  $232\text{s}$ . With a naïve boustrophedonic scan the beam will turn around and return in the opposite  $x$ -direction  $0.025\text{m}$  displaced in  $y$ . When the beam reaches the edge of the segment it runs off it some distance, then moves up and turns around. This time off the segment serves no purpose, so should be done as quickly as practical. The distance the beam needs to move is no more than about four sigma. The flux is down by about 3000 from the central flux, so the removal rate on the segment is very near to zero. If the beam goes off this amount, and goes up 1 sigma, then returns, the motion is  $0.225\text{m}$ , and takes  $\sim 44\text{s}$  if the beam speed is not changed from  $0.005\text{m/s}$ . If the  $xy$  stage moves at maximum speed ( $0.25\text{m/s}$ ) the turnaround will take under  $2\text{s}$ .

Thus when the beam returns, it will heat up a strip whose centerline is  $0.025\text{m}$  apart (in  $y$ ) from the previously heated  $x$  scan line. Figure 11 shows the overlap of Gaussians separated by 1 sigma. Clearly the overlap is large,  $\sim 0.9$ , so the overlap in  $y$  will cause almost doubling of the surface temperature when the time between strips is small compared to the lateral thermal diffusion time constant of  $396\text{s}$ . At 2 sigma separation the overlap is more than 50%, so there will still be significant overlap heating.

The scan pattern should be adjusted to basically eliminate overlap heating and to distribute the power as quickly and evenly as practical over the entire segment in order to maximize radiative cooling. We see no particular downside to have the adjacent scans be far apart other than the time spent moving the beam back to the beginning for the next scan.

We suggest that consecutive strips be separated by five sigma. At this spacing the additional heating is under 5%. This is somewhat arbitrary, but workable. For our segment it will take  $1.16/.125=9.28$  strips to cover the mirror. This will take  $2.15e3$  seconds. Then the process needs to be repeated 4 more times with 1 sigma offsets to cover the entire mirror with 1 sigma spacing. This will take  $1.08e4$  seconds. This entire process needs to be repeated 12.2 times (total time is 36.6 hrs) to achieve the desired bulk removal of  $0.5\mu\text{m}$ .

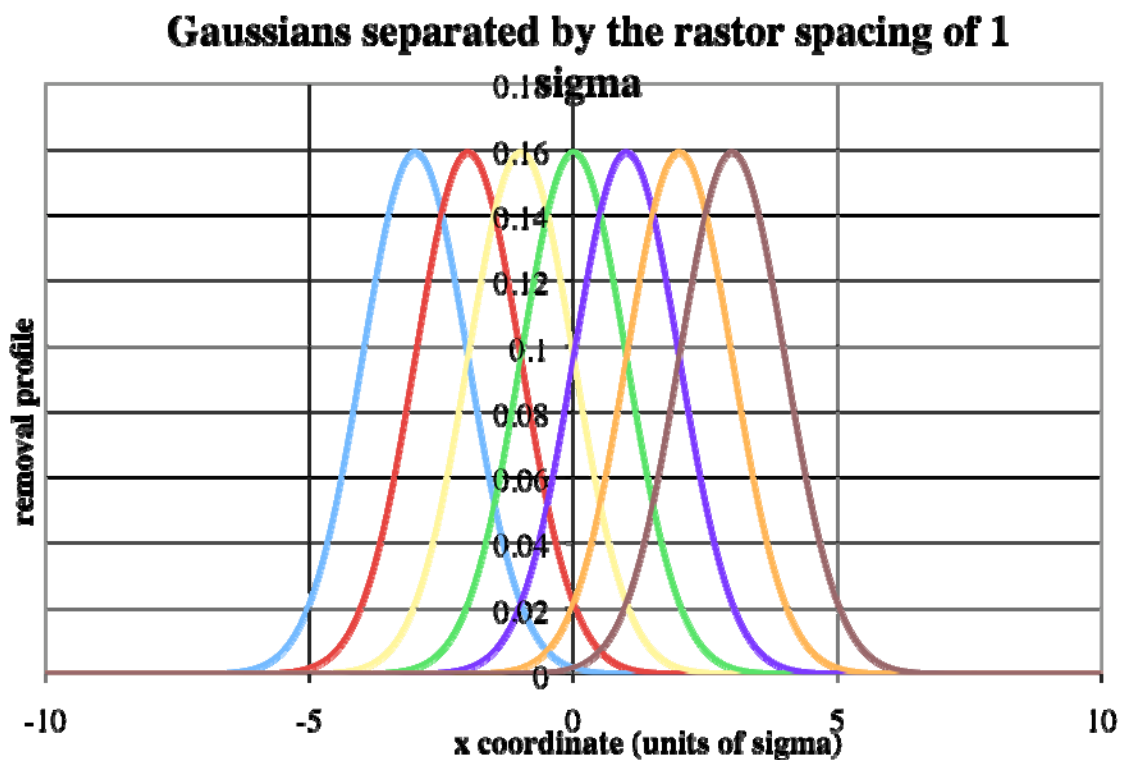


**Figure 11** Gaussians separated by 1 sigma.

An example of the scan pattern is shown schematically in Figure 12. For the example a uniform speed would be used to remove  $0.5\mu\text{m}$  uniformly over the segment. Each scan pattern is shifted by  $0.025\text{m}$  from the last, and each scan pattern has its rows displaced by  $0.125\text{m}$ . For the desired removal volume the scan must be repeated  $\sim 12$  times. In reality the beam speed will vary to achieve the desired spatially variable over the segment surface.

The aim of the suggested scan pattern is to spread out the heat deposited over the segment, in order to take maximal advantage of the radiative cooling of the segment. There are a number of different patterns that might be used to achieve this while minimizing the local heating.

Real removal will not be uniform of course, but will depend on the polishing and warping errors that a given segment has experienced. In extreme cases where there is a very localized high

region that requires removal, special care may be needed to avoid overheating such a local region.

Given the minimum speed of 0.005m/s and the maximum xy stage speed of 0.25m/s, we will remove about 2% unnecessary material in the low regions. Although this is a modest effect, a proper removal algorithm should take this into account.

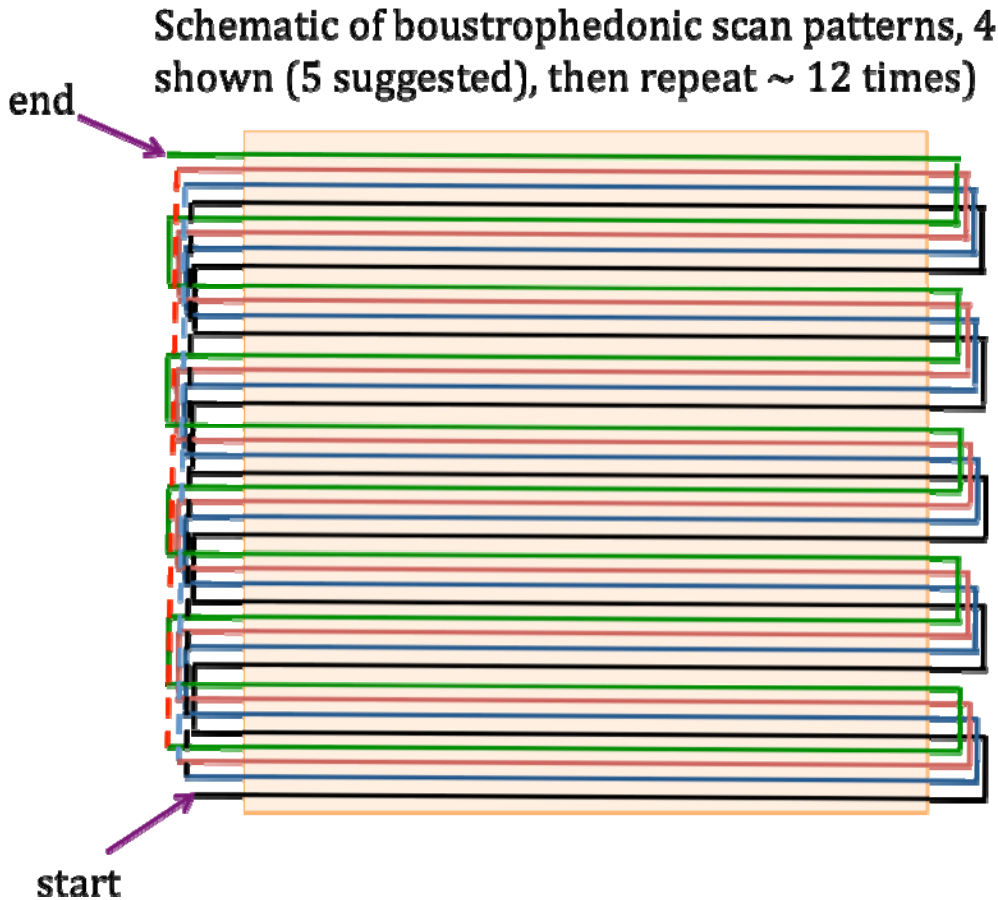


**Figure 12** A schematic of a boustrophedonic scan pattern to IBF a segment. Four patterns are shown (black, blue, red, green). The text recommends 5 such patterns. The entire set of patterns is to be repeated ~ 12 times to achieve the example 0.5 $\mu$ m uniform removal of glass from the segment. Note on the left the return to the next pattern is shown as dashed lines. For a real segment the pattern would be as suggested, but the scan speed will vary depending on the material to be removed.

## 7 Comparison with Finite Element Analysis

Given the complexity of the problem and the calculations, it is worthwhile checking some of the results against a finite element thermal model. Even FEA calculations can be difficult to set up then the input conditions vary with time. As a result we have limited our comparison to a few simple cases. We thank Jerry Cabak for carrying out the FEA calculations.

### 7.1 Heat dumped at the surface, Gaussian distribution

We calculate for a circular disk the temperature rise along the z axis caused by 126 Joules of energy deposited in a Gaussian pattern on the  $z=0$  surface, centered at  $x=y=0$ . This is the

situation described by (14). We calculate this for two times,  $t=100s$  and  $t=600s$ . The FEA and the analytic results are shown in Figure 13. They show good agreement.

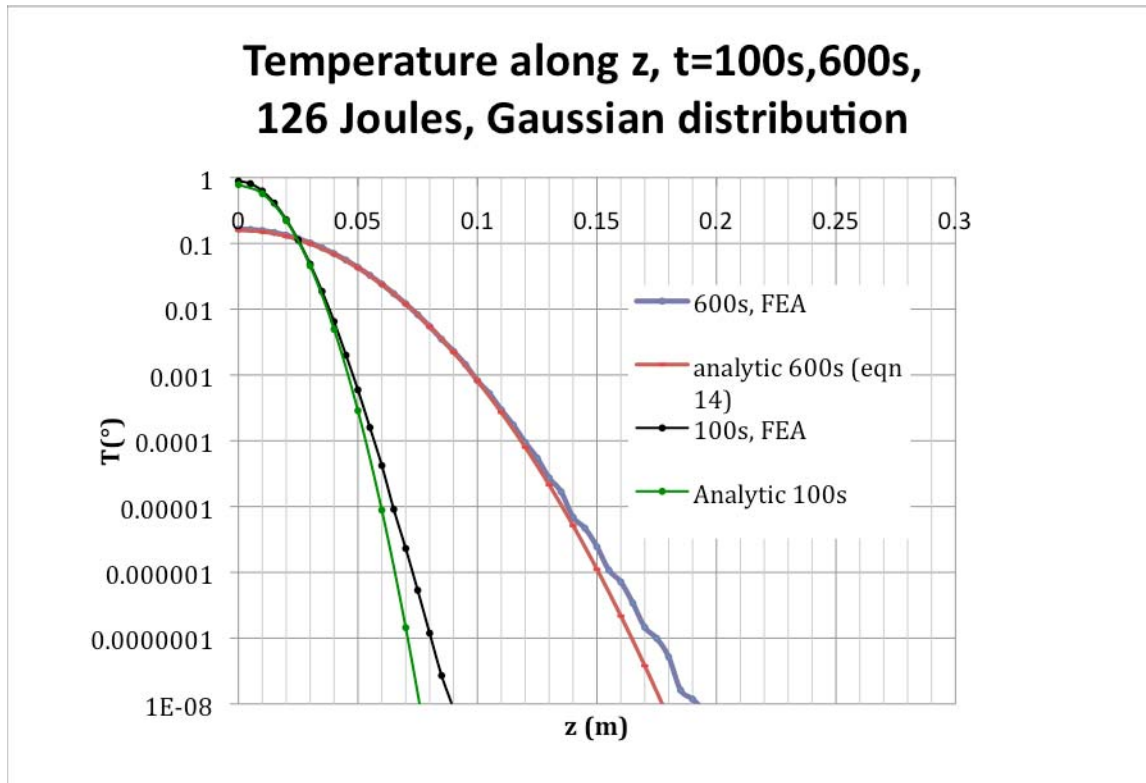


**Figure 13** The temperature distribution along  $z$  is shown for two times,  $t=100s$  and  $t=600s$  for 126J deposited at  $z=0$ , in a Gaussian pattern. The analytic and the FEA calculations are in good agreement, confirming (14)

## 7.2 Power Deposited at Surface, Resulting Surface Heating

We calculate for a circular disk the increase in surface temperature at  $(0,0,0)$  when a Gaussian beam with power  $P=126$  impinges on the surface of the segment. This problem is solved analytically in (16). The FEA results and the analytic results are shown in Figure 14. The mesh size of the FEA model is varied and the plate thickness is varied. These variations have only modest effect, and the results are in good agreement with the analytic model. The plate thickness of 20mm produced no significant change compared to a very thick plate.

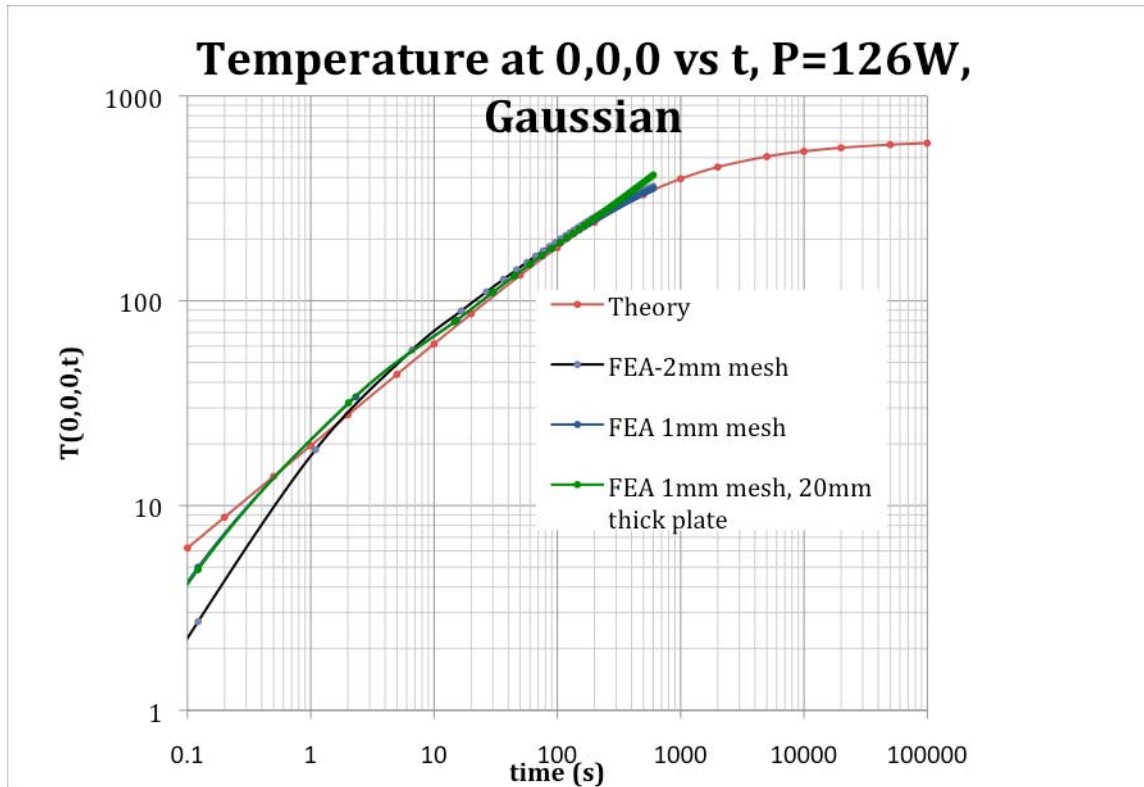


**Figure 14** The temperature at (0,0,0) as a function of time is shown. Constant power ( $P=126\text{W}$ ) is deposited in a Gaussian shape with  $\sigma=0.025\text{m}$  on the top surface. The results are in good agreement with the analytic model (16). The impact of a finite thickness ( $h=20\text{mm}$ ) has little effect on the results.

## 8 Possible experiments

Given the difficulty of these calculations and the importance of not overheating the mirror, it is worthwhile carrying out experiments with a sample of glass and the actual ion beam in the chamber. We suggest a few experiments.

1. Using a piece of glass roughly  $0.4\text{m} \times 0.4\text{m} \times 0.045\text{m}$  in size, place a thermocouple in the center at the surface. Perhaps a small hole bored through the mirror with the thermocouple installed as close as practical to the front surface would work, but it may be possible to simply attach it directly to the surface. Apply the beam to the center of the mirror and monitor the temperature rise over a duration of 10s. The temperature rise should agree with (17). Then turn the beam off and monitor the temperature for the next 2000s. It should match the temperature fall off predicted by (14).
2. Scan the ion beam across the width of the mirror at  $v=0.005\text{m/s}$  and monitor the surface temperature at the center of the mirror. The temperature should match the predictions of (20).
3. Scan the beam across the mirror in a pattern similar to that suggested in 6.4. Repeat this for  $\sim 10,000\text{s}$ . The temperature should rise, and reach steady state temperature balance between the ion beam power in and the radiative power out. This should

follow (9) or (10). The scan speed may need to be much faster than 0.005m/s to avoid the local heating added to the global temperature rise damaging the bond.

It may be useful to place thermocouples on the back surface as well as the front. If the thermocouple is bonded to the front surface, care must be taken not to overheat the adhesive holding the thermocouple. If the effort is minor, it will also be interesting to place multiple sensors along the scan line in experiment 2 and directly check (20).

## 9 Summary

We have shown that a segment subject to IBF will, on average, radiate away the power from the IBF gun to the chamber walls, and this will cause only modest heat rise. However, the local heating from the gun (assumed  $P=126W$ , Gaussian beam profile  $\sigma=0.025m$ ) will cause excess heating ( $\Delta T > 50^\circ$ ) if the beam is stationary for more than 7sec. If the beam is moving at a constant velocity, the speed must be  $> 0.005m/s$  to avoid damage from excess local heating. At the maximum slew rate of 0.25m/s, the removal rate can vary a factor of 50 from the fastest to the slowest speeds. Thus removal efficiency is significantly compromised.

We have developed a simple algorithm for IBF that will efficiently remove all low spatial frequency errors. The algorithm varies the speed of the ion gun while leaving its power constant.

Our analytic predictions have been checked against an FEA model with good agreement. Nonetheless we suggest several experiments to strengthen our confidence in our understanding.

We have given an example of a beam scan pattern that avoids any excess local heating and allows the global radiation to limit the heat rise, so the segment can be ion beam figured safely at full power.

-----

Note: This version has been reviewed and approved by concerned parties 6/28/2010.